

Topography Characterization and Initial Cellular Interaction of Plasma-Based Ar⁺ Beam-Treated PDMS Surfaces

I. Keranov,¹ T. G. Vladkova,¹ M. Minchev,² A. Kostadinova,³ G. Altankov,³ P. Dineff⁴

¹Department of Polymer Engineering, University of Chemical Technology and Metallurgy (UCTM), 1756 Sofia, Bulgaria

²Central Laboratory of Photoprocesses, Bulgarian Academy of Sciences, 1113 Sofia, Bulgaria

³Institute of Biophysics, Bulgarian Academy of Sciences, 1113 Sofia, Bulgaria

⁴Department of Electrical Apparatus and Technologies, Technical University (TU), 1756 Sofia, Bulgaria

Received 10 January 2007; accepted 23 April 2008

DOI 10.1002/app.29185

Published online 2 December 2008 in Wiley InterScience (www.interscience.wiley.com).

ABSTRACT: Assuming that the existence of an ion-flow in the plasma volume could strengthen the surface modifying effect, including its durability, a parallel plate reactor in reactive ion etching mode was employed to obtain surface modified PDMS with improved cellular interaction. The discharge power was varied at 100, 1200, and 2500 W to ensure varied ion-flow density. The changes in the surface topography were observed by SEM and AFM, and the surface roughness was characterized by both: mean roughness, R_a , and root-mean-square, R_q . Time dependent water contact angle measurements were performed to control the durability of the hydrophilizing effect. Anisotropic etching, accompanied with decrease of the PDMS

surface roughness, was observed up to discharge power of 1200 W that turns in intense isotropic one, accompanied with a sharp increase of the surface roughness over 1200 W, most probably because of arise of reverse sputtered neutrals diffracting the main plasma Ar⁺ flow. Human fibroblasts were applied as an *in vitro* model to learn more about the initial cellular interaction of the modified surfaces and to identify the optimal treatment conditions. © 2008 Wiley Periodicals, Inc. *J Appl Polym Sci* 111: 2637–2646, 2009

Key words: polysiloxanes; cold plasma; nanolayers; AFM; hydrophilic polymers

INTRODUCTION

Polymeric materials are not specifically recognized by living cells¹ that limits their biomedical applications. Therefore, surface modification techniques creating suitable chemistry, topography, and wettability have become a key approach toward the tailoring of their biological properties.² In this respect, the plasma treatment is one of the most widely used methods. For example, cold plasma obtained in low pressure glow discharge has been applied to activate polymer surfaces, including siloxane membranes,^{3–6} for further grafting of monomers as AA, HEMA, etc. aimed at rendering the surface hydrophilicity and improvement of their interaction with living cells. Ion-beam is another way to amend the biocon-

tact properties of materials, particularly of poly(hydroxyl-methylsiloxane) (PHMS),^{7,8} an effect confirmed by us also at poly(dimethylsiloxane) (PDMS) surface.^{9,10} Assuming that the existence of an ion-flow in the plasma volume could strengthen the surface modifying effect, including its durability, a parallel plate reactor in reactive ion etching mode (RIE) was employed to obtain surface modified PDMS with improved cellular interaction. The discharge power was varied at 100, 1200, and 2500 W (corresponding to surface density of the discharge power of: 0.55 W/cm²; 1.1 W/cm² or 2.2 W/cm², respectively) to ensure different ion-flow density.

A partial characterization of PDMS surfaces treated under the above conditions was presented in previous our publication.¹¹ Now, we continue this investigation focusing mainly on the influence of plasma-based Ar⁺ beam treatment on the surface morphology, topography, and roughness observed by SEM and AFM, as well as, on the correlation with the initial cellular interaction *in vitro*. A well-defined human fibroblasts cell model was applied for the later studies, and the surfaces were pretreated with fibronectin (FN) to ensure optimal cellular response. Further characterization of the

Correspondence to: T. G. Vladkova (tgv@uctm.edu).

Contract grant sponsor: Ministry of Education and Science, Bulgaria (Polymeric Materials with Nanosize Modifying Layers); contract grant number: NT 2-04/2004.

Contract grant sponsor: National Fund Scientific Investigations.

biocompatibility, cell growth, and the ability of fibroblasts to organize their own FN matrix were monitored and explored according to previously described studies.^{12,13}

EXPERIMENTAL

Samples preparation

PDMS thin films (thickness of 50–70 μm) were deposited on prelyophilized cover glasses (15 mm \times 15 mm) by spinning of Silopren LSR 2070 (FDA, GE Bayer Silicones) precursor polymer solution in toluene (5% v/v) and cured in conventional way.

Plasma-based Ar⁺ beam treatment

The samples were treated in plasma-based Ar⁺ beam performed in RF (13.56 MHz) low-pressure (200 mTorr) glow discharge with a serial capacitance described in detail.¹¹ The treatment duration was of 1 min, and the discharge power was varied at 100, 1200, or 2500 W (surface density of the discharge power of: 0.55, 1.1, or 2.2 W/cm², respectively).

Contact angle measurement

Modified method of Bickerman^{14–16} was used to evaluate the static contact angle of two liquids with known surface tension¹⁷: polar H₂O ($\gamma_{\text{lv}} = 72.8$ mJ/m², $\gamma_{\text{lv}}^d = 21.8$ mJ/m² and $\gamma_{\text{lv}}^p = 51.0$ mJ/m²) and nonpolar CH₂J₂ ($\gamma_{\text{lv}} = 50.8$ mJ/m², $\gamma_{\text{lv}}^d = 49.5$ mJ/m² and $\gamma_{\text{lv}}^p = 1.3$ mJ/m²) measuring the diameter of three drops of each volume: 1, 2, and 3 μL . Surface free energy and their components were calculated according to Kaelble's equation.^{14,17–20}

SEM observation

The surface morphology of the nontreated and modified PDMS surfaces was observed with SEM, Philips-515.

AFM

AFM in tapping mode (AFM device: Nanoscope-3, Digital instruments, Santa Barbara, CA) using a single crystal silicon probe (model TESP) with a spring constant of 0.58 N/m was employed to obtain more detailed information about the surface topography and roughness. The scanning frequency was of 1 Hz.

Mean roughness, R_a (nm) was calculated using the following equation:

$$R_a = \frac{1}{L_x L_y} \int_0^{L_y} \int_0^{L_x} [f(x, y)] dx dy$$

where, L_x and L_y are dimensions of the surface.

Root-Mean-Square, R_q (nm) was calculated as a standard deviation of the Z values within the given area as shown:

$$R_q = \sqrt{\frac{\sum (Z_i - Z_{\text{ave}})^2}{N}}$$

where, Z_{ave} is the average of the Z -values within the given area Z_i ; Z_i current Z value; N number of points within given area.

Cells

Human fibroblasts were prepared from fresh skin biopsy and used up to the 9th passage. The cells were grown in Dulbecco's minimal essential medium (DMEM) containing 10% fetal bovine serum (FBS) (Sigma Chemicals Co., St. Louis, MO) in a humidified incubator with 5% CO₂. For the experiments, the cells were harvested from nearly confluent cultures with 0.05% trypsin/0.6 mM EDTA (Sigma).

Initial cellular interaction

The initial cellular interaction was characterized by monitoring the overall cell morphology of fibroblasts adhering for 2 h on above surfaces precoated with FN. Briefly, 15 mm \times 15 mm samples prepared as above were placed in 6-well TC plates (Costar) and washed three times with PBS. All samples were precoated with FN (see below). 3×10^5 cells per well were added and incubated for 2 h in humidified CO₂ incubator at 37°. Then, the samples were viewed at 20 \times magnifications on the inverted phase contrast microscope (type Fluoval 20, Zeiss, Germany) equipped with digital camera.

Fibronectin preparation

Human plasma FN was prepared by affinity chromatography on gelatin-Sepharose 4B²¹ and further purified on heparin-Sepharose 4B. Later, the FN was eluted with 0.5M NaCl, 50 mM Tris pH 7.3 and lyophilized. For the experiments, FN was dissolved in distilled water at a concentration of 1 mg/mL and stored at 4°C for up to 1 week. Working dilutions were done in PBS. Surfaces were precoated with FN by incubation with 20 $\mu\text{g}/\text{mL}$ for 30 min at 37°C. Then, the samples were washed three times with PBS prior to adding the cells.

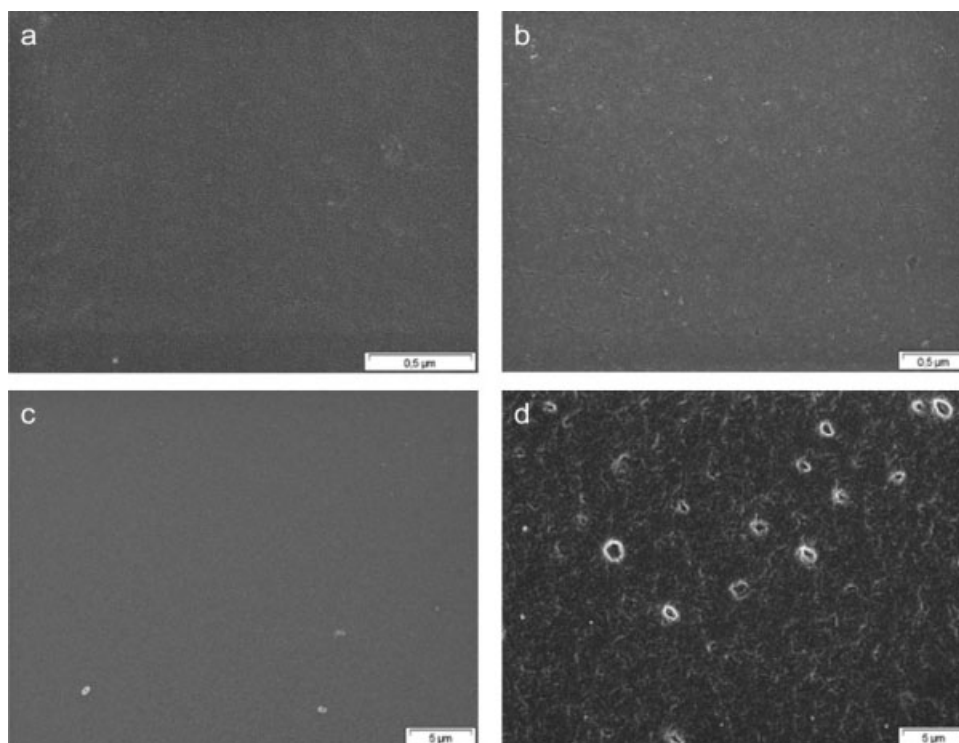


Figure 1 SEM images of PDMS surfaces: nonmodified (a) and plasma-based Ar⁺ beam treated for a constant time of 1 min and at varied discharge power of 100 (b), 1200 (c) and 2500 W (d).

Immunofluorescence for FN matrix

To study FN matrix formation, human fibroblasts were cultured for 3 days in 6-well TC plates containing the samples at initial seeding density of 1×10^5 cells per well. Then, samples were washed with PBS, fixed for 5 min with 3% paraformaldehyde (in PBS), and saturated for 15 min with 1% bovine serum albumin (BSA) (Sigma). To visualize FN, the samples were incubated for 30 min at room temperature with anti-FN monoclonal antibody (Sigma Cat. No F 7387) diluted 1 : 100 in 1% BSA in PBS followed by Cy2 conjugated goat anti mouse secondary antibody (Dianova, Germany) 1 : 100 in 1% goat serum in PBS. Finally the samples were washed three times in PBS, mounted in Moviol, and viewed on the fluorescence microscope (Fluoval 20) using the green (FITC) channel. The images were captured with CCD camera.

Cell proliferation assay (LDH)

The cell proliferation was determined via modified lactate dehydrogenase (LDH) assay (Hoffman La Roche, Penzberg, Germany) after 1, 3, and 5 days of incubation. The LDH assay is a colorimetric method originally developed for the quantification of cell death based on the measurement of LDH activity released from the cytosol of damaged cell. We applied this system to measure the enzymatic activity after total cell lyses, thus, quantifying the total amount of cells and hence cell proliferation (30N), as

previously described.²² Briefly, at the indicated incubation time, the medium was removed and the cells were lysed with 0.5 mL 1% Triton-X 100 in PBS under shaking for 1 h. The cells lysates were centrifuged at $2000 \times g$ for 5 min. Thereafter, 100 μ L of LDH test solution was added to each well, and the samples were incubated for 15 min at room temperature in dark. The reaction was stopped with 50 μ L 1M HCl. The absorbance was measured with Spectra Flour Plus plate reader (Tecan, Crailsheim, Germany) at 492 nm. The reference wavelength was at 620 nm. Each experiment was quadruplicated.

RESULTS AND DISCUSSION

Surface topography and roughness

SEM observation of the surface of nonmodified and plasma-based Ar⁺ beam-treated PDMS showed the picture, presented in Figure 1(a–d). As it is evident from this figure, the surface of the PDMS samples treated at 100 [Fig. 1(b)] and 1200 W [Fig. 1(c)] as well as the nontreated PDMS [Fig. 1(a)] seems to be very smooth, whereas that of the sample treated at 2500 W [Fig. 1(d)] demonstrates specific morphology.

AFM study was performed by us to obtain more detailed information about the surface structure of the same samples. Surface topography of the nonmodified PDMS as well as its altering as a result of the plasma-based Ar⁺ beam treatment are revealed by 3D

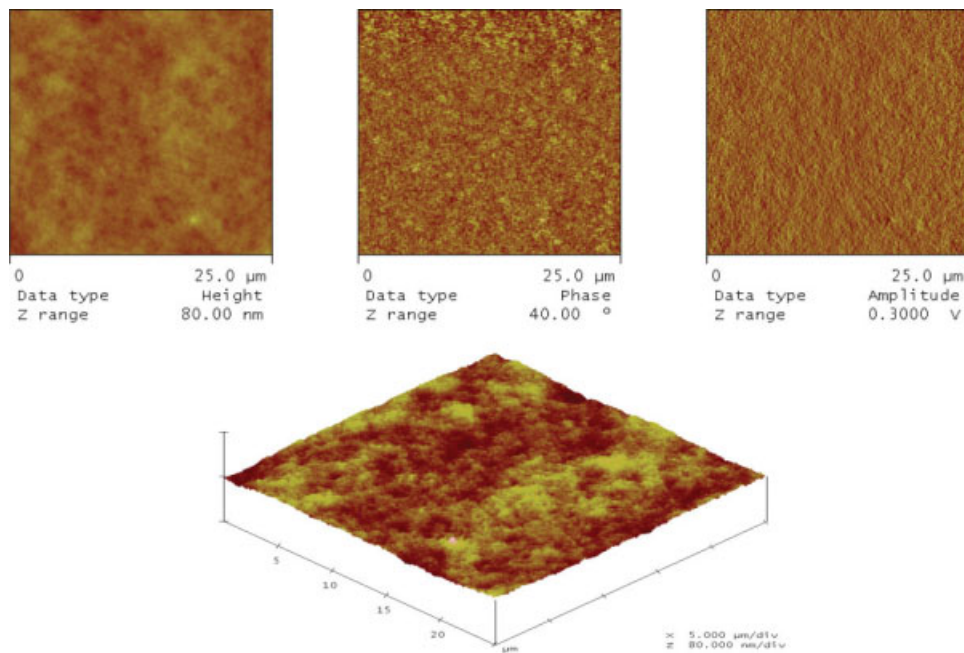


Figure 2 AFM images of nonmodified PDMS surface: 2D height (a), phase (b) and amplitude (c); 3D height (d). [Color figure can be viewed in the online issue, which is available at www.interscience.wiley.com.]

and top AFM images represented in Figures 2–5. The surface roughness parameters R_a and R_q are further calculated and compared (see Table I).

The control untreated sample (see Fig. 2) has relatively smooth— $R_a = 1.593$ nm; $R_q = 2.013$ nm (Table I, row 1) and small-grain surface topography, similar to that observed by other authors.²³ This small-grain surface topography is kept almost the same after treatment at low discharge power (of 100 W), Figure 3.

Evidently, the treatment under these conditions causes mainly surface ablation leading to the formation of large but not depth valleys and, respectively, to some decrease of the surface roughness when compared to that of the nontreated PDMS (Table I, compare row 2 with row 1): R_a get down to 1.284 and R_q to 1.656.

The ablation is more pronounced at the PDMS sample treated at a discharge power of 1200 W

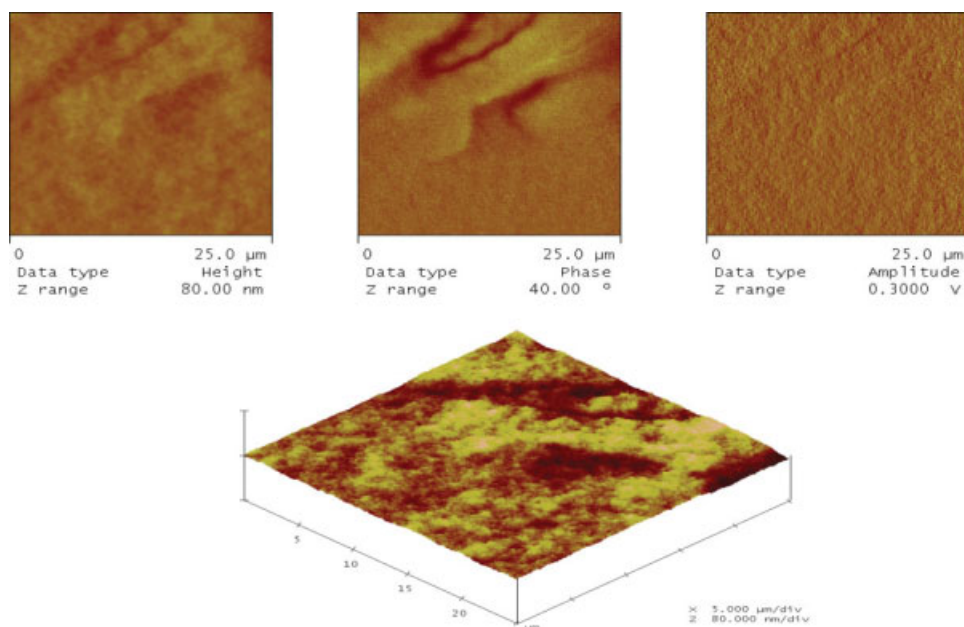


Figure 3 AFM images of PDMS surface plasma-based Ar^+ beam treated for a constant time of 1 min and a discharge power of 100 W: 2D height (a), phase (b) and amplitude (c); 3D height (d). [Color figure can be viewed in the online issue, which is available at www.interscience.wiley.com.]

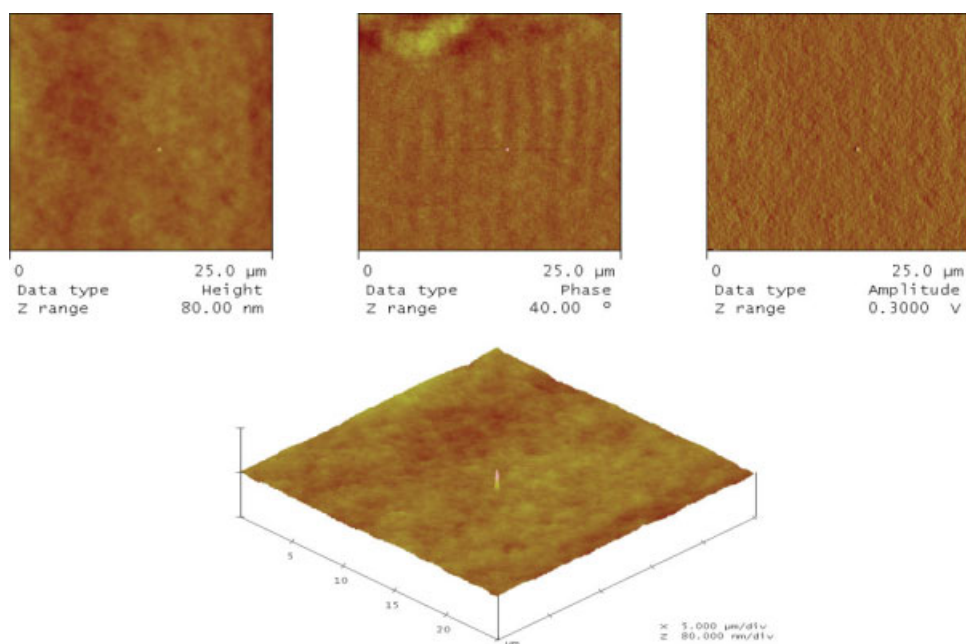


Figure 4 AFM images of PDMS surface plasma-based Ar⁺ beam treated for a constant time of 1 min and a discharge power of 1200 W: 2D height (a), phase (b) and amplitude (c); 3D height (d). [Color figure can be viewed in the online issue, which is available at www.interscience.wiley.com.]

(Fig. 4). Its surface is smoother compared to that of both: the nonmodified (Fig. 2) and treated at a lower discharge power (of 100 W, see Fig. 3) PDMS samples. Correspondingly, the surface roughness continues to get down: R_a and R_q become 1.201 and 1.064, respectively (Table I, row 3).

As it is evident from Figure 5, the 2D and 3D images are quite different if the plasma-based Ar⁺ beam is performed at a higher discharge power (of 2500 W): domains are formed, clearly seen in all 2D images of the treated sample, thought to be due to some mineralization of the starting PDMS (SiO_x

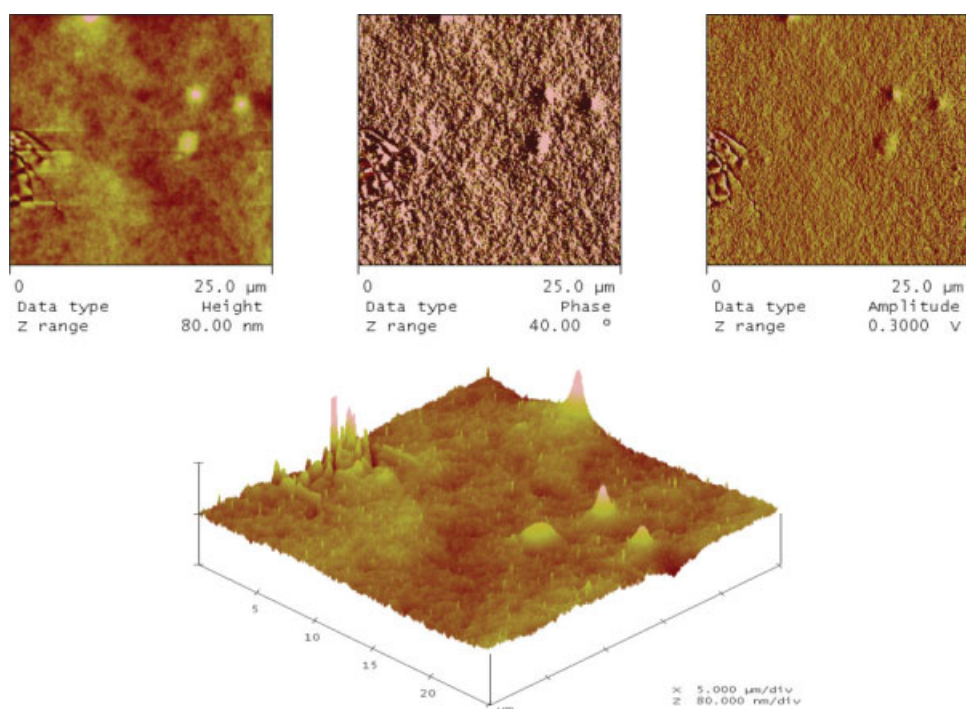


Figure 5 AFM images of PDMS surface plasma-based Ar⁺ beam treated for a constant time of 1 min and a discharge power of 2500 W: 2D height (a), phase (b) and amplitude (c); 3D height (d). [Color figure can be viewed in the online issue, which is available at www.interscience.wiley.com.]

TABLE I
Mean Roughness, R_a , and Root-Mean-Square Roughness, R_q , of Nonmodified (Control) and Plasma-Based Ar^+ Beam-Treated PDMS for 1 min at Different Discharge Powers: 100, 1200, and 2500 W

Sample	Scan size (μm)	R_a (nm)	R_q (nm)
PDMS nonmodified	25	1.593	2.013
PDMS treated at 100 W	25	1.284	1.656
PDMS treated at 1200 W	25	1.201	1.064
PDMS treated at 2500 W	25	3.868	5.808

phase formation), earlier detected by XPS analysis.¹¹ The 3D image of the same sample [Fig. 5(d)] shows a large number of small peaks and some large peaks and valleys, which are missing on the control non-treated PDMS surface [Fig. 2(d)] as well as on the surfaces treated at a lower discharge power [of 100 W, Fig. 3(d) or of 1200 W, Fig. 4(d)]. Most probably, these peaks are of the mineralized phase that is more stable to the Ar^+ beam.

In addition, an effect of anisotropic etching accompanied with decrease of the PDMS surface roughness is observed up to 1200 W, which most probably is turned in an intense isotropic etching, accompanied with a sharp increase of the surface roughness over 1200 W due to arise of reverse sputtered neutrals diffracting the main plasma Ar^+ flow, as it is described for other cases of similar treatment.²⁴

Surface hydrophilization and its durability

Surface hydrophilization of the PDMS was expected due to the change of both: (i) the surface roughness and (ii) the surface chemical composition as a result of the plasma-based Ar^+ beam treatment. Several parameters, presented in Table II, were used by us to evaluate this effect. The data in Table II clearly demonstrate the expected surface hydrophilization, better expressed when the treatment is performed at higher discharge powers:

The water contact angle, $\theta_{\text{H}_2\text{O}}$ of the strongly hydrophobic nonmodified PDMS of 101.9° decreases down to 87.9° , 60.8° , and 39.4° for the PDMS samples treated at a discharge power of 100, 1200, and 2500 W, respectively. This decrease of the water contact angle, $\theta_{\text{H}_2\text{O}}$ is accompanied with a correspond-

ing increase of the surface energy, γ_s (from 22.9 mJ m^{-2} for the nonmodified PDMS up to 57.1 mJ m^{-2} for the sample treated at discharge power of 2500 W) and polarity (from 0.05 for the nonmodified PDMS up to 0.68 for the sample treated at discharge power of 2500 W), mainly due to the increase of the polar component of the surface energy, γ_s^p (from 1.1 mJ m^{-2} for the nonmodified PDMS up to 38.7 mJ m^{-2} for the sample treated at a discharge power of 2500 W). The observed hydrophilization of the strong hydrophobic nonmodified PDMS could be explained with both: the altering of the surface chemical composition, earlier registered by us with XPS analysis¹¹ and the above described change of the surface topography. Plasma-based Ar^+ beam treatment of the PDMS leads to accumulation of O-containing polar groups on its surface whose amount increases with the increase of the discharge power up to 1200 W,¹¹ Table I and correspondingly, the water contact angle decreases (Table II). It should be noted that the surfaces of the samples treated at discharge power of 1200 and 2500 W, in spite of their very similar chemical composition,¹¹ Table I demonstrate quite different hydrophilicity, thought to be such due to their quite different surface topography and roughness.

It is well known that the plasma-treated polymer surfaces undergo surface reconstruction just after the treatment tending to approach their starting properties. On the other hand, it has been found that the surface modifying effect of the ion-beam^{7,8} is stable during a long time. Expecting that the durability of the plasma-based Ar^+ beam modifying effect will increase when compared to that of the conventional plasma treatment, we performed a measurement of the water contact angle of all studied samples during a long time interval: 30 min–720 h. The experimental results are represented in Figure 6.

As it is evident from Figure 6, the water contact angles of all treated PDMS samples are lower than the water contact angle of the strong hydrophobic nonmodified PDMS (101.9°) and they are lower than 90° immediately after the treatment as well as after 720 h (30 days) storage at room conditions indicating the stable turning of their surface into hydrophilic one. Changes of the water contact angle are

TABLE II
Static Contact Angles, $\theta_{\text{H}_2\text{O}}$ and $\theta_{\text{CH}_2\text{I}_2}$, Surface Energy, γ_s , and its disperse, γ_s^d , and Polar, γ_s^p , Components as well as the Surface Polarity, p , of Different PDMS Surfaces

Sample	$\theta_{\text{H}_2\text{O}},^\circ$	$\theta_{\text{CH}_2\text{I}_2},^\circ$	$\gamma_s \text{ (mJ m}^{-2}\text{)}$	$\gamma_s^d \text{ (mJ m}^{-2}\text{)}$	$\gamma_s^p \text{ (mJ} \cdot \text{m}^{-2}\text{)}$	Polarity (p)
PDMS nonmodified	101.9	70.2	22.9	21.8	1.1	0.05
PDMS treated at:						
100 W	87.9	66.7	26.8	21.9	4.95	0.18
1200 W	60.8	49.5	45.6	28.1	17.5	0.38
2500 W	39.4	61.8	57.1	18.5	38.7	0.68

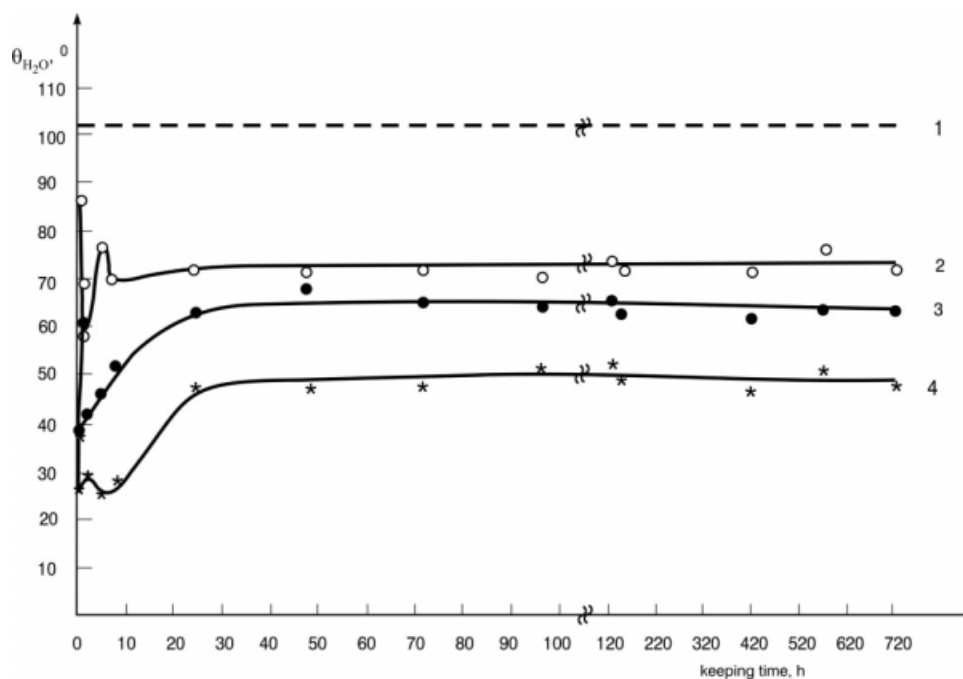


Figure 6 Dependence of the water contact angle, $\theta_{\text{H}_2\text{O}}$ on the keeping time at room conditions for different PDMS surfaces: nonmodified—curve (1); plasma-based Ar⁺ beam treated at a constant time of 1 min and a varied discharge power of 100 (curve 2), 1200 (curve 3) and 2500 W (curve 4).

observed for all plasma-based Ar⁺ beam treated samples in the first 24 h (Fig. 6, curves 2, 3, and 4). This indicates an existence of some surface reorganization during this time. After that, the water contact angle of all treated surfaces is almost constant indicating that the surface reconstruction is completed in the first 24 h. In addition, the water contact angle of all treated samples stay far lower than 90° demonstrating that the observed surface reconstruction can not turn the modified surfaces back to hydrophobic and they retain the hydrophilicity for a long time. Evidently, their hydrophilicity depends on the plasma-based Ar⁺ beam treatment conditions: as higher is the discharge power during the treatment as lower is the water contact angle (Fig. 6, compare curves 2, 3, and 4).

Initial cellular interaction

The data presented up to now show that the plasma-based Ar⁺ beam treatment alters simultaneously several surface parameters of the treated PDMS, which could affect the initial cellular interaction: the chemical composition,¹¹ hydrophilic/hydrophobic balance (Table II and Fig. 6), and the surface topography and roughness (Figs. 2–5), which in turn depend on the treatment conditions and especially on the discharge power.

Overall cell morphology

The overall cell morphology of fibroblasts adhering for 2 h on control nonmodified sample (a) and plasma-based Ar⁺ beam treated PDMS surfaces (b, c, d) is presented in Figure 7. It is evident that the number of fibroblasts on the nonmodified, strong hydrophobic ($\theta_{\text{H}_2\text{O}} = 101.9^\circ$) PDMS surface is less, and they represent round shape because of the disturbed cell spreading. Conversely, both cell adhesion and spreading are positively influenced on the treated samples. On the slightly hydrophilic PDMS surface ($\theta_{\text{H}_2\text{O}} \cong 73^\circ$, Fig. 6) created by treatment at low discharge power (of 100 W), the cells look much better spread. About half of the fibroblasts develop their typical flattened morphology with an extended cell shape. This effect is presumably connected with the noted hydrophilization of the surface, although some changes of its chemical composition also exist.¹¹ The decreased surface roughness (see Table I) may also play a role despite here we have similar to control small-grain topography (Figs. 2 and 3).

The treatment at higher discharge power, (1200 W) however, leads to an increase of the surface hydrophilicity ($\theta_{\text{H}_2\text{O}}$ get down to about 65°, Fig. 6), does not improve significantly the cellular interaction [Fig. 7(c)] although a bit less round shaped cells are observed. It is interesting to notice that this sample characterizes also with the smoothest surface: $R_a = 1.201$ nm and $R_q = 1.064$ (Table I), which implies

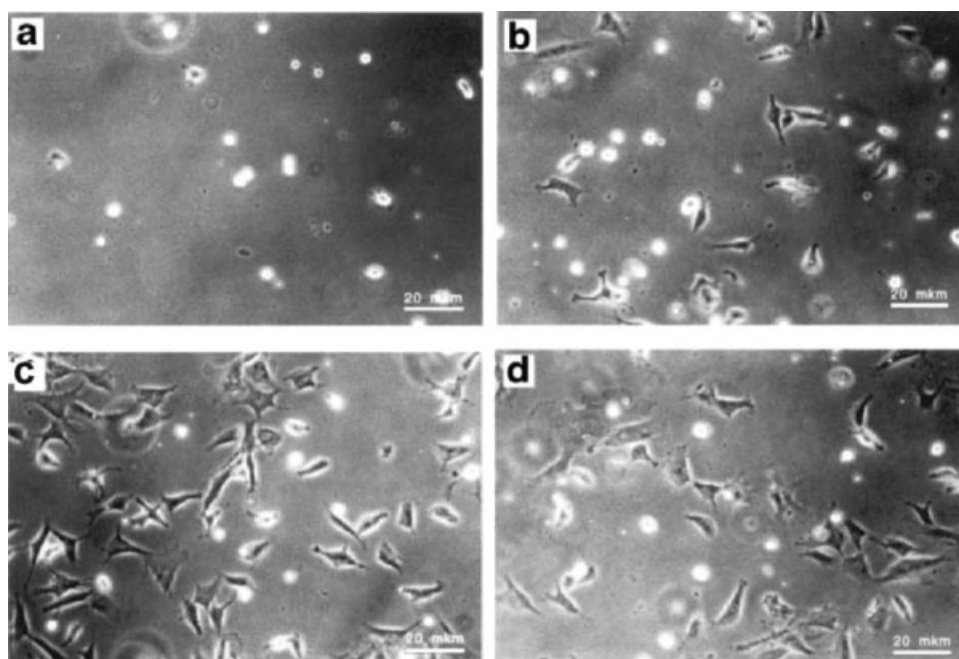


Figure 7 Overall morphology of human fibroblast cells on different PDMS surfaces: nonmodified (a) and plasma-based Ar^+ beam treated at a constant time of 1 min and a varied discharge power of 100 (b), 1200 (c) and 2500 W (d).

that changes in this range of both wettability and roughness do not play significant role.

The best initial cellular interaction was observed on the surface treated at a discharge power of 2500 W [Fig. 7(d)]. The number of cells here is significantly higher and the relative amount of nonspread fibroblasts is less. It is noteworthy that this surface characterizes with the lowest water contact angle ($\theta_{\text{H}_2\text{O}} \cong 50^\circ$, Fig. 6) and the highest roughness ($R_a = 3.868$ nm, $R_q = 5.808$, Table I). According to some authors,²⁵ however, the best cellular interaction might be expected at surfaces with water contact angle of about 60° . Consequently, our PDMS surface treated at 2500 W should not be better compared to that treated at 1200 W ($\theta_{\text{H}_2\text{O}} \cong 65^\circ$). Therefore, the improved initial cellular interaction has to be attributed rather to the increased roughness. Although controversial results exist, it is generally well documented that the nano-scale surface roughness affects the interactions with cells.²⁶

Cell growth

The capability of different plasma-based Ar^+ beam treated PDMS samples to support the cell growth over a period of 7 days was studied using LDH assay. As illustrated in Figure 8, the plasma-based Ar^+ beam treatment tend to increase the cell growth. The last one is significantly higher for the 3rd and 7th day at the samples treated at discharge power 1200 or 2500 W. This effect evidently depends on the treatment conditions: it is weak on the PDMS sam-

ple treated at a discharge power of 100 W and it increases with the increase of the discharge power up to 2500 W. This partly corroborate the observed better cellular interaction, particularly on the later (2500 W) sample. Therefore, it is reasonable to assume that the successful initial cellular interaction with the substratum is a prerequisite for the generation of adequate signals to the cell interior that finally triggers the DNA replication machinery. Nevertheless, the cell growth is clearly depressed on the nonmodified PDMS surface, which correlates with the literature,²⁷ and imply on the fact that we got a successful approach for the surface treatment. However, we could not see again correlation with

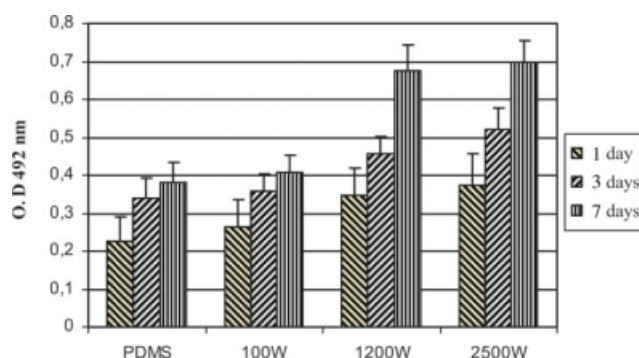


Figure 8 Capability of different PDMS surfaces (nonmodified and plasma-based Ar^+ beam treated at a constant time of 1 min and a varied discharge power of 100, 1200, and 2500 W) to support cell growth over a period of 7 days using the LDH assay. The treated surfaces promote an increased cell growth at each day of incubation.

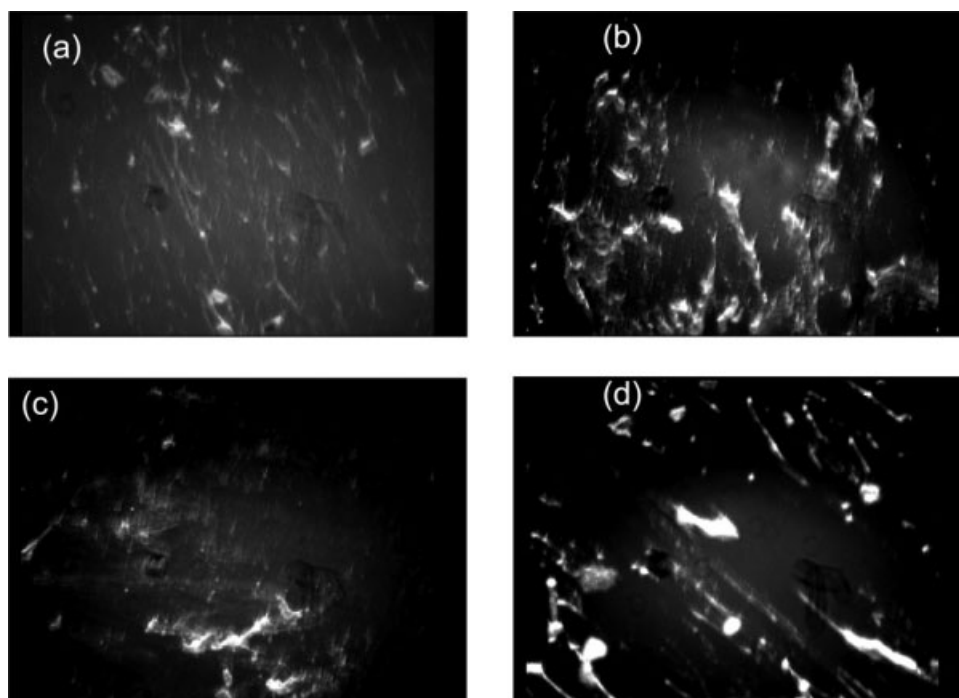


Figure 9 Cell immunofluorescence for human fibroblast cells fibronectin matrix formation on different PDMS surfaces: nonmodified (a) and plasma-based Ar^+ beam treated at a constant time of 1 min and a varied discharge power of 100 (b), 1200 (c) and 2500 W (d).

the “optimal” wettability of the surfaces, as it is worse on the sample treated at discharge power of 100 W. As for the chemical composition of surfaces, which also could change the cells proliferation response, we have to admit that the samples treated at discharge power of 1200 and 2500 W characterize with almost the same chemical composition and quite different morphology and surface roughness (Figs. 4, 5, and Table II). Thus, the significantly improved cell growth on the sample treated at 2500 W, when compared to that treated at 1200 W (Fig. 8), consequently might be attributed to the strongly increased surface roughness.

Fibronectin matrix formation

A main function of fibroblasts *in vivo* is to synthesize and organize ECM in a specific 3D meshwork consisting of fibrillar matrix proteins, such as collagen, laminin, FN, and proteoglycans.²⁸ This organization of ECM can be studied also *in vitro* and particularly relevant approach is to follow the formation of FN matrix fibrils by cultured fibroblasts. It is clearly shown that FN matrix deposition is strongly affected on the material surface properties.²⁹ One surface parameter that clearly influences FN matrix formation is the surface wettability. The hydrophobic materials alter or completely block this process, presumably as a result of the stronger protein interaction with the surface.^{12,25} As it can be seen from Figure 9, our

results show that fibroblast FN matrix formation is altered on plain PDMS surface, an effect presumably connected with its hydrophobicity. Conversely, the Ar^+ beam treatment tends to improve the FN matrix formation following the trend of increasing surface hydrophilicity, but it seems not obligatory, as on PDMS treated at discharge power of 1200 W, the altered deposition of fibrillar FN is clearly visible. Nevertheless, fibroblast organize better FN matrix on plasma-based Ar^+ beam treated surfaces, particularly at discharge power of 100 and 2500 W, which suggests relatively weak adsorption strength for FN, an indirect measure for a relatively good biocompatibility at cellular level.¹³

CONCLUSIONS

Plasma-based Ar^+ beam treatment of poly(dimethylsiloxane) alters its surface topography and roughness as proven by SEM and AFM.

Lasting hydrophilization of the poly(dimethylsiloxane) surface due to an increase of the surface polarity was proven as a result of such treatment, this effect depending on the discharge power.

In addition, the plasma-based Ar^+ beam treatment improves the poly(dimethylsiloxane) initial interactions with leaving cells, this effect is better pronounced when the treatment is performed at higher discharge power: of 1200–2500 W.

No direct correlation was found between the surface hydrophilicity and the initial cellular interaction presumably is due to the simultaneous influence of other factors like surface chemical composition and roughness.

The surface treatment at discharge power of 2500 W is the most promising regarding the initial cellular interaction and especially the extra cellular matrix formation.

GKSS Institut für Chemie, Teltow, where AFM was performed is gratefully acknowledged.

References

1. Ratner, B. D. *Macromol Symp* 1998, 130, 327.
2. Rana, N.; Sodhi, S. *J Electron Spectrosc Relat Phenom* 1996, 81, 269.
3. Chan, C. M.; Ko, T.-M.; Hiraoka, H. *Surf Sci Rep* 1996, 24, 1.
4. Abbasi, F.; Mirzadeh, A.; Katbab, A.-A. *Polym Int* 2001, 50, 1279.
5. Chu, P. K.; Chen, J. Y.; Wang, L. P.; Huang, N. *Mater Sci Eng* 2002, R36, 143.
6. Lee, Sh-D.; Hsiue, G-H.; Kao, Ch-Y. *J Polym Sci A: Polym Chem* 1996, 34, 141.
7. Satriano, C.; Conte, E.; Marletta, G. *Langmuir* 2001, 17, 2243.
8. Satriano, C.; Carpanza, S.; Guglielmino, S.; Marletta, G. *Langmuir* 2002, 18, 29469.
9. Vladkova, T.; Keranov, I.; Dineff, P.; Altankov, G. *Proceedings of the 4th International Conference of the Chemical Societies of the South-Eastern European Countries (ICOSECS 4)* 18-21 July 2004, Belgrad, Serbia, p 629.
10. Vladkova, T.; Keranov, I.; Dineff, P.; Altankov, G. *Proceedings of the XVIIIth Congress of the Chemists and Technologists of Macedonia*, 21-25th September 2004, Ohrid, Macedonia, p 16.
11. Vladkova, T.; Keranov, I.; Dineff, P.; Youroukov, S.; Avramova, I.; Krasteva, N.; Altankov, G. *Nucl Instrum Methods Phys Res* 2005, B236, 552.
12. Groth, Th.; Altankov, G. *J Biomater Sci Polym Ed* 1995, 7, 297.
13. Altankov, G.; Grinnell, F.; Groth, Th. *J Biomed Mater Res* 1996, 30, 385.
14. Chan, Ch-M. *Polymer Surface Modification and Characterization (SPE Book)*; Hanser Publishers, 1994.
15. Garbassi, F.; Morra, M.; Occiello, O. *Polymer Surfaces from Physics to Technology*; Wiley: Chichester, UK, 1994.
16. Bikerman, J. J. *Ind Eng Chem* 1941, 13, 443.
17. Morra, M.; Occiello, O.; Marola, R.; Grabassi, F.; Humphrey, P.; Johnson, D. *J Colloid Interface Sci* 1990, 137, 11.
18. Kaelble, D. H. *Adhesion* 1970, 2, 50.
19. Ho, C-P.; Yasuda, H. *J Appl Polym Sci* 1990, 39, 1541.
20. Inagaki, N.; Tasaka, S.; Hibi, K. *J Polym Sci A: Polym Chem* 1992, 30, 1452.
21. Fowkes, F. M. *Ind Eng Chem* 1964, 56, 40.
22. Vladkova, T.; Krasteva, N.; Kostadinova, A.; Altankov, G. *J Biomater Sci* 1999, 10, 609.
23. Chen, H.; Brook, M. A.; Scheardown, H. *Biomaterials* 2004, 25, 2273.
24. Hippler, R.; Pfau, S.; Schmidt, M.; Schönbach, K. H., Eds. *Low Temperature Plasma Physics, Fundamental Aspects and Applications*; Wiley-VCH: Berlin, 2001.
25. Altankov, G.; Groth, Th. *J Mater Sci Mater Med* 1994, 5, 732.
26. Catapano, G.; Di Lorenzo, M. C.; Volpe, C. D.; De Bartolo, L.; Migliaresi, C. *J Biomater Sci Polym Ed* 1996, 7, 1017.
27. Park, J. H.; Bae, J. H. *J Biomed Mater Res* 2003, 64, 309.
28. Wilson, J.; Hunt, T. *Molecular Biology of the Cell*, 4th ed; Garland Sci: New York, 2002; p 223.
29. Midwood, K. S.; Mao, Y.; Hsia, H. C.; Valenik, L. V.; Schwarzbauer, J. E. *J Invest Dermatol Symp Proc* 2006, 11, 73.
30. Tamada, Y.; Kulik, E. A.; Ikada, Y. *Biomaterials* 1995, 16, 295.